Manuscript of the article: Microporous and Mesoporous Materials 167 (2013) 109-116
http://dx.doi.org/10.1016/j.micromeso.2012.03.011

Cu and Cu_2In nanoparticles supported on amorphised zeolites for the selective reduction of biomass derived carboxylic acids to alcohols

Szabolcs Harnos, György Onyestyák, Dénes Kalló

Institute of Materials and Environmental Chemistry, Research Centre for Natural Sciences, Hungarian Academy of Sciences, Pusztaszeri u. 59-67, Budapest, Hungary, 1025

Abstract

Octanoic acid (OA) was used as reactant with medium chain length to model the aliphatic carboxylic acids which can be produced by catalytic, thermochemical or biological degradation of biomass. A flow through reactor was applied at 21 bar total pressure (in general at 20 bar hydrogen and 1 bar octanoic acid partial pressures) and 330-380 °C. Cu A-, X- and Y-zeolite based catalysts were pretreated in hydrogen flow at 450 °C. During reduction/dehydration A- and X-zeolite structures collapsed and aluminosilicate supported copper catalysts were formed, which contain copper nanoparticles in high dispersion. The catalyst samples were modified by In_2O_3 co-catalyst. Fatty acid conversion activity of amorphized zeolite supported Cu catalysts and the yield of selectively produced alcohol can be increased drastically by In_2O_3 addition. Appearance of metallic indium can effectively rein in the step by step catalytic reduction at alkanol formation previous to dehydration of alcohols to alkenes and ethers.

Keywords: Biomass, Fatty acids, Hydroconversion, Cu-zeolites, Alcohols; In_2O_3 doping

INTRODUCTION

The forthcoming shortage of fossil energy resources and the environmental problems force more extensive utilization of the biomass to produce chemicals and fuels. There are attempts to adopt petrochemical technologies for biomass processing. However, because the crude oil and the biomass are fundamentally different raw materials, novel conversion methods, new catalysts are needed. Without deep upgrading the use of bio-oils obtained from various sources as transportation fuel is very limited [1]. The biomass-derived oils, such as, e.g., the vegetable or pyrolysis oils are free of S but contain O in high concentration. The bio-oils can be upgraded to high-quality transportation fuel by decreasing its heteroatom, mainly O content using catalytic hydrotreatment [2-4] which results in formation of alkanes.

From the early 1930s the chemical industry transforms triglycerides, primarily vegetable oils, by catalytic hydrogenation to fatty alcohols. Large amounts of fatty acids can be produced by stopping the fermentation of biomass after the fast anaerobic acid formation and before the slow methanogenesis [5]. The well-known catalyst to produce alcohols selectively from carboxylic acids or esters is the generally used copper chromite (Adkins catalysts) at 250-300 °C and 250-300 bar. This catalyst consists of an approximately equimolar mixture of cupric-oxide CuO and cupric chromite $CuCr_2O_4$ [6]. Copper catalysts enable the selective addition of hydrogen to carbon-oxygen bonds but are less active in the hydrogenolysis of the carbon-carbon bonds [7]. The chromium promoted copper catalysts show high activity and selectivity for alcohol formation. However, because the high pressure and the use of chromium raises environmental concerns, research is focused to develop chromium-free catalysts (e.g., a series of Mo, Co, Zn, Mn, Fe, Y, Ni, Mg promoted Cu/SiO_2 catalysts [7]) for the ester conversion to alcohols under milder conditions. Evans et al. [8] showed that copper on silica, or even pure Raney copper, can be as effective as copper chromite for the

hydrogenolysis of esters to alcohols. The finely dispersed metallic copper seems to be the catalytically active component in these systems for hydroconversion of fatty acids or the esters. Regularly structured crystalline microporous aluminosilicates, like X- and P-zeolites were supposed to be suitable supports for the stabilization of well-dispersed active copper clusters [9]. Fatty acid hydroconversion and the yield of selectively produced alcohol can be increased drastically by In_2O_3 doping. Appearance of metallic indium can effectively direct the step by step catalytic reduction to alcohol formation over partly reduced Ni catalysts instead of chain shortening hydrodecarbonylation [10].

The objective of this work is to develop method for the selective reduction of carboxylic acids to alcohols over novel catalysts. Depending on the molecular mass of the carboxylic acid to be converted obtained alcohol is either long chain or short chain fatty alcohol. Short chain alcohols, like ethanol, can be obtained by microbial fermentation of sugar and starch but conversion of edible sources is not the appropriate way to produce fuels and chemicals in the future. However, various, cheap, inedible biomass raw materials can be effectively transformed in high volume by anaerobic digestion to carboxylic acids [11-13], which can then be converted to alcohols by catalytic hydrogenation. Long chain fatty alcohols which can be produced with lower hydrogen consumption than hydrocarbons from waste fats and oils may be admixed to gasoil, too. The present study compares the features of selective carboxylic acid hydroconversion to alcohol using octanoic acid (OA) as a model reactant of medium chain length over three different, indium promoted Cu/aluminosilicate catalysts obtained from zeolite A (small pore) and faujasites (zeolite X or Y, large pore) having different frameworks but consisting of the same building units (linked truncated octahedras, β-cages) and being of similar composition in A and X.

EXPERIMENTAL

Catalyst preparation

Copper-zeolites A, X and Y were prepared from NaA (Baylith), NaX or NaY (products of the late VEB CKB, Bitterfeld-Wolfen, Germany) powders, respectively. Si/Al ratios were approx. 1 for zeolite A and X, 2.6 for Y. Cu-forms were obtained by conventional aqueous ion-exchange with Cu (II) acetate (purity >99%, from Merck) solutions, liquid to solid weight ratio of about 10. The amount of Cu^{2+} in the solutions was about equivalent to the ion-exchange capacity of the zeolites resulting in 15-16 wt.% Cu^{2+} content for zeolite A and X, and 7 wt.% Cu^{2+} for zeolite Y. The slurries were stirred at room temperature for two times 8 h with fresh solution in each period. After washing the materials were dried at room temperature. Al, Na and Cu contents of the zeolites were determined by Atomic Absorption Spectroscopy (AAS) with Varian Spectra A20 atomic absorption spectrometer.

Activated industrial silica-alumina (SiAl), having a Si to Al ratio of 6.6 was impregnated with Cu(II)acetate to obtain 20Cu/SiAl catalyst with 20 wt.% Cu content. For the designation of the preparations the symbol of the element copper (Cu) is used, followed by the name of the support such as CuA, CuX, CuY or Cu/SiAl. The number before the symbol Cu represents the metal content of the samples, expressed in weight percent. Main catalyst characteristics are summarized in Table 1.

Composite catalysts were prepared by adding indium (III) oxide (99.99% purity, Aldrich) to the Cu-containing samples and grinding the mixture in agate mortar.

Catalyst characterization

X-ray patterns were recorded with a Philips PW 1810/1870 diffractometer applying monochromatic Cu K_α radiation (40 kV, 20 mA) at elevated temperatures using a high-temperature XRD cell (HT-XRD). The mean crystallite size of the copper particles was

estimated by the Scherrer equation with XDB Powder Diffraction Phase Analytical System program using profile fitting method for the determination of the full-width at half-maximum (FWHM) of the copper reflections [14].

Nitrogen physisorption measurements were carried out at -196 °C using Quantochrome Autosorb 1C instrument for determination of specific surface areas.

The reducibility of the Cu^{2+} cations in the samples was investigated by temperature-programmed reduction (H_2-TPR) in H_2/Ar flow using a conventional TPR apparatus equipped with a heat conductivity detector. About 250 mg catalysts were pretreated in a flow of 20 ml/min N_2 gas at 400 °C for 1 h, then cooled to room temperature in the same gas stream. The pretreated samples were contacted with a 20 ml/min flow of 9.6 v/v % H_2/Ar gas mixture at room temperature. The sample temperature ramped up to 800 °C at the rate of 10 °C/min and maintained at final temperature for 1 h. The extent of copper reduction was determined by the hydrogen consumption of the samples.

Catalyst activity measurements

The catalytic hydrogenation of octanoic acid (OA) (purity ≥98%, from Aldrich) was carried out in a high-pressure fixed bed flow reactor generally at 20 bar H_2 pressure, 1 bar OA pressure, WHSV of OA = 2.0 h^{-1} (standard conditions) and 330-380 °C. The experimental setup is illustrated in Fig. 1. The inner diameter of the microreactor is 16 °mm, the height of catalyst bed is 120 mm. In this reactor the longitudinal diffusion is negligible under the reaction conditions. The prepared powders were pressed without binder to pellets and applied as catalysts in form of crashed particles 0.63-1.00 mm in size. Before reaction all the catalysts were activated in 230 ml/min pure hydrogen flow in situ in the reactor at 21 bar H_2 and 450 °C for 1 h. Thereafter the system was cooled down to the desired reaction temperature then the appropriate feed was started. When the dependence on partial pressure of reactants was studied an OA/H_2/He flow of appropriate composition was introduced at 21 bar total

pressure. The reaction was allowed to run one hour at each temperature to attain steady state. Before taking sample, the effluent during the second hour was collected, depressurized and cooled to room temperature.

A commercial, conventionally used Adkins catalyst (consisting of 72 wt.% $CuCr_2O_4$ and 28 wt.% CuO) was tested for comparison with the novel catalyst preparations.

Product analysis

The product mixtures were analyzed by GC (Shimadzu 2010) equipped with a CP-FFAP CB capillary column and a flame ionization detector. The gaseous reactor effluent was analyzed for CO_2, CO, CH_4 and light hydrocarbons, and traced using an on-line GC, Carboxen 1006 PLOT capillary column (30 m x 0.32 mm), and thermal conductivity detector. In the figures output compositions in wt% of components are plotted as stacked area graphs, where the distance between the curves represents the concentration of a component in the effluent.

RESULTS AND DISCUSSION

Structural changes of catalysts (BET, FTIR, H_2-TPR and HT-XRD results)

The H_2-TPR (Fig. 2) and the HT-XRD (Fig. 3) results suggest that in the zeolite based catalysts, activated before the reaction at 450 °C in H_2 flow for one hour, all the copper was present in finely dispersed metal particles: In the H_2-TPR apparatus the reduction of copper starts at about 200 °C and finishes at about 450 °C for CuX and at about 700 °C for CuA as shown in Figs. 2a and 2A. The hydrogen consumption for metallic copper formation is found near to 1 H_2/Cu mol/mol. Under conditions of HT-XRD measurements (the linear heating up is interrupted with half hour long constant temperature steps) complete copper reduction comes to an end at much lower temperature (350 °C) than the routine pretreatment temperature (450 °C) as shown in Fig. 3. On increasing the temperature from 350 °C to 450 °C Cu^0 line intensities do not change either as for CuA or as for CuX.

However, these zeolite structures are amorphized at significantly different temperatures up to the pretreatment temperature. Consequently differences both in H_2-TPR curves and XRD patterns can be observed for CuA and CuX. In contrast, the structure of CuY is completely preserved up to 450 °C in the HY form containing intact Brönsted acidity and the distinct Cu^0 metallic phase.

During the TPR measurements, the admixed nonporous, compact, large crystals of the In_2O_3 separate phase (accessible for reducing agent only on the tiny outer surface) can be completely reduced only at higher temperature than highly dispersed copper ions originally bound homogenously to cationic sites of microporous zeolites. Furthermore the course of indium III oxide reduction seems to be influenced by the differences of zeolite structures affected the In_2O_3 dispersion, the interaction of the oxide and the aluminosilicate phases. XRD patterns of the composite catalyst samples (Fig. 3A, B, C) show that above 350 °C diffraction lines of In_2O_3 disappear: at higher temperature for A- than for X- (or Y-) zeolite. The destructed Cu-zeolite catalysts treated at 450 °C have specific surface area of 8 m^2/g for CuA and 18 m^2/g for CuX that is the surface area is low in comparison with the 221 m^2/g surface area of the non-zeolitic based, as well amorphous 20Cu/SiAl catalyst used for comparison.

On zeolite dehydration and reduction of charge compensating Cu^{2+} cations the zeolite A or X structure sorely damaged below 250 °C as recorded in XRD patterns. CuA is already completely collapsed up to 350 °C recorded to be fully amorphous in XRD patterns. CuX can preserve some crystallinity up to 450 °C. The reason is that the dehydration of the zeolite catalyst containing bivalent copper cations, as well as the reduction of the cations with hydrogen leads to the formation of H-zeolites being unstable at such a low Si/Al ratio [15]. Regarding the structural instability towards dehydration and H_2 reduction zeolites CuX and CuA seem to behave similarly because of the similar chemical composition, similarly low

silicon/aluminum ratio (approx. 1). However in spite of similarities the structural differences of zeolites are demonstrated by different temperature dependence of the zeolite destruction. Significant differences can be observed in the series of CuX HT-XRD patterns on increasing temperature using helium or hydrogen flow. Brönsted acid sites formed in helium during dehydration by heterolytic dissociation of cation bound water molecules in the strong electrostatic field of bivalent cations can occupy only the half of all the cationic sites presently in the field of Cu^{2+} ions. Since not negligible fraction of structure seems to be preserved the deeply damaged structure may be more or less permeable.

Thermogravimetric measurements (TG, DTG, DTA, curves are not shown here) demonstrate complete sameness in dehydration behavior of CuX and CuA having the same zeolitic building units but connected differently. In spite of this observation during dehydration different destructed supports (showed in XRD patterns) for the active metal clusters are formed. FTIR spectra of Fig. 4 reflect the different extent of remaining Brönsted acidity of the pretreated supports. NH_4X zeolite pretreated at 450 °C in H_2 flow resulting in collapse of the H-zeolite structure obtained during deammonization can preserve significant amount of Brönsted acidity contrary to NH_4A indicated by spectra after pyridine adsorption where the band of pyridinium ion at 1545 cm^{-1} appears. This observation is in agreement with XRD results which show that CuX gives weak diffraction lines at high pretreatment temperature when Cu-A became totally X-ray amorphous (Fig. 3).

The diffraction lines, assigned to metallic copper phase were evaluated between 200 and 350 °C for CuX and CuA (cf. a and b diffractograms in Fig. 3). Thus, the metal clusters could be formed when the zeolite structure had already been deeply damaged. The size of copper clusters has important relevance. The widths of the diffraction lines assigned to Cu^0 particles are strikingly different in Fig. 3 for the hollow CuX and the more compact CuA. Consequently, the average copper particle sizes in CuX and in CuA are 26 nm and 7 nm,

respectively. In CuY, where in the stable faujasite framework copper cations have free access for the reducing agent hydrogen and the formed copper atoms can migrate to the surface of the zeolite crystals without barrier the average copper particle size is larger, 55 nm. The largest copper particles, having an average diameter of 98 nm formed in the 20Cu/SiAl catalyst. In this catalyst the specific surface area of the support is the largest and that of the copper metal is the smallest among all the studied catalysts.

XRD patterns of the composite catalyst samples (Fig. 3A, B, C) show that at 450 °C In_2O_3 lines completely disappear indicating total reduction, however cooling to room temperature, i.e., far below the melting point of indium (156.4 °C), indium metal particles can not be detected. It seems likely that small copper particles should be able to form CuIn alloy. Thus In^0 diffraction lines can only be detected after cooling the samples to R.T when copper clusters on the support are not present. After reduction liquid indium (being its melting point 156.4 °C) is formed and spread over the solid surface. New lines at a bit lower Bragg angles than the most intense line of copper at 43.3° appear in the diffractograms which can be assigned to some kind of CuIn alloy [14], mainly to Cu_2In phase. This phase determined based on ICDD database, the corresponding ICDD number was Cu_2In: 42-1475. It can be concluded: if the catalyst contains enough reduced metallic copper clusters (some are not detectable because of small size), the total mass of indium which is reduced at lower temperature can form CuIn alloy and thus In^0 diffraction lines can not appear after cooling to R.T. The shape and intensity of the diffraction lines assigned to Cu_2In phase are different for zeolites X and A reflecting the different structure of precursor.

Conversion of octanoic acid over the base Cu-catalysts

The activity and selectivity of the catalysts studied can be characterized by the product distributions as function of reaction temperature represented in stacked area graphs for CuA

and CuX (Fig. 5a and b) of near the same composition show hardly different activity but strikingly different selectivity. The difference of surface areas seems to have no relevance in the hydroconversion because the supports are practically inactive under these conditions and the activity can thus be ascribed to copper clusters. (Parent Na-forms of crystalline zeolite A and X proved to be inactive up to 380 °C. Destructed NH_4-A and –X show some activity above 350 °C only and can form similarly 1 % octanol and 8 % octene at 380 °C which amounts are negligible compared to those found for Cu catalysts under identical conditions.) The commensurable conversions over these differently destructed Cu-zeolite catalysts with similar chemical composition cannot be perfectly interpreted yet, since composition, structure, concentration of active sites are not known. The stable CuY zeolite structure with lower Al- and Cu-contents and much bigger Cu^0 particles of much less metal surface shows significantly lower conversion and very poor selectivity.

Octanal (that intermedier produced in the first step of fatty acid reduction series) yields (AL) are similarly low over all the studied catalysts. The catalyst CuA was the most selective for alcohol (OL) formation, i.e. the relative yields of octanol to octane are strikingly different over the zeolite based catalysts under similar conditions. When the reaction temperature was increased the octene yield increased on the expense of the octanol yield. This change was much more pronounced over the CuX and mainly CuY than over the CuA catalyst (cf. Figs. 4a, b and c), i.e., CuA shows essentially lower dehydration activity than CuX and especially CuY. It is interesting that although the starting zeolites are built up of the same building units (sodalite cages), the destruction of structure (detected by XRD technique) results in strikingly different residual Brönsted acidity, specific surface area and copper nanocluster surfaces consequently the selectivities or relative rates of the consecutive reduction and dehydration steps are different:

$$\text{octanoic acid} \xrightarrow[-H_2O]{+H_2} \text{octanal} \xrightarrow[-H_2O]{+H_2} \text{octanol} \rightarrow \text{octenes} \xrightarrow{+H_2} \text{octane}$$

Observed differences reflect that these catalysts have different structural features in nanometer scale.

As for comparison, a real industrial amorphous silica-alumina catalyst (Fig. 5d) having the highest activity (cf. the concentrations of not-converted OA in Fig. 5) shows only extremely low alcohol selectivity, producing mainly the final products of the above reaction scheme. Beside octenes ($C_8^=$) and octane (C_8) heptene olefins ($C_7^=$) and paraffines (C_7) can also be observed due to hydrodecarbonylation of octanal when in the gas phase CO can be detected, as well. The high dehydration activity can be attributed to significant Brönsted acid site concentration spread on the much larger specific surface area than destructed zeolites have similarly to CuY sample which works as HY catalyst loaded with large copper metal parlicles.

Conversion of octanoic acid over the In doped Cu-catalysts

Adding In_2O_3 to all four Cu-catalysts (Fig. 5A, B, C, D) the main effect is that activity increases (not-converted OA concentrations are lower) and octanol yields increase significantly while octene yields decrease, although for the 7CuY and 20Cu/SiAl catalyst the influence is only modest. The effect of indium seems to be complex. The relatively higher increase of AL content and relatively lower increase of OL content indicates increase of hydrogenation activity in higher degree for AL formation and relatively to lower degree for OL formation. Presumably a copper-indium alloy formation (Fig. 3) is responsible for activity increase since it has been found that the activity of reduced In_2O_3 is negligible under these conditions. Another question is how and why is suppressed the dehydration activity by the appearance of metallic indium atoms on the surface of support and/or metal particles.

The efficiency of a commercial, conventionally used Adkins catalyst (consisting of 72 wt.% $CuCr_2O_4$ and 28 wt.% CuO) was compared with the novel catalyst preparations containing Cu_2In nanoparticles under identical conditions (see Table 2). The new, chromium free CuA + In_2O_3 composite seems to be slightly less active which is reflected by the hardly lower conversion but much higher octanal yield. Accumulation of the less reduced intermediate product, octanal can demonstrate the less activity of Cu_2In alloy surface or the smaller size of the active surface compared to the interactions over the copper chromite catalyst. Adjusting more efficient reaction conditions (e.g. longer contact time resulting in higher conversion even at lower reaction temperature, see in last row of Table 2.) similar excellent alcohol yield and selectivity can be attained as with the environmentally very harmful conventional chromium type catalyst. There is an open room for fruitful catalyst developments applying novel indium doping method in various hydrogenation catalysts [10] by varying the supports and active metals.

Effects of reaction parameters

Fig. 6 demonstrates the influence of space time at two temperatures on the product distributions over the less selective CuX mixed with In_2O_3 co-catalyst. Consecutive hydrogenation and dehydration reaction steps are clearly reflected: The longer the space time the lower the AL, the higher the OL formation and the octene yield appearance is.

OL yields increase with hydrogen partial pressure and AL yields decrease (Fig. 7) as expected for the consecutive hydrogenation conversion at the same space time. In Fig. 8/a p_{H2} dependence is shown at lower temperature on In_2O_3 doped CuA catalyst. Due to lower activity AL concentration is considerably higher than OL concentration. Fig. 8/b demonstrates the conversions as function of p_{OA}. The shape of curves indicates the strong adsorption of OA suppressing hydrogen which results first in increase thereafter in decrease of conversion. Langmuir-Hinshelwood kinetics seems likely.

The role of indium as alloy forming metal

Fig. 9 reveals that AL is hydrogenated much faster on CuA than on CuA+In_2O_3 (similarly as shown in Fig. 5a-A). The aldehyde is observed to be much more reactive than carboxylic acid in the hydrogenation reaction (well-known fact from organic chemistry). The hydrogenation of OA on indium containing catalyst is faster than on CuA (cf. Fig. 5a-A) but the hydrogenation of AL is faster when indium is not present (cf. Fig. 5a-A, Fig.9 a-b). This shift of hydrogenation selectivities may be attributed to the copper indium alloy being presumably a new catalytically active phase. The reason of simultaneously suppressed not desirable alcohol dehydration by indium is not clear yet.

It has been found that even 3 % In_2O_3 additive deeply influences the catalytic behavior of conventionally pretreated CuX and CuA catalysts. In the range of high amount of In_2O_3 additive negligible changes can be observed (Fig. 10). Taking into account that metallic copper particles are present after reduction and small amount of reduced (but single inactive) In_2O_3 decisively influence the catalytic properties, Cu-In alloy on Cu surface forming detectable crystals seems to create the active sites.

CONCLUSIONS

Highly dispersed copper particles can be generated on aluminosilicate supports formed by destructive H_2 reduction/dehydration of zeolite CuA and CuX. Such amorphised CuA and CuX type catalysts show high activity and selectivity in the catalytic hydroconversion of carboxylic acids to alcohols. The selectivity to alcohol depends on the original zeolite structure. Zeolite CuA (small pore) seems to be a better catalyst precursor than CuX (large pore), having the same composition but different frameworks consisting of the same building units (linked truncated octahedras). The activity and the alcohol yield of the supported Cu catalysts can be effectively increased by In_2O_3 doping. Appearance of indium metal in the

active metallic copper containing phase highly increases the activity and the selectivity. It seems likely that indium suppresses the dehydration of octanol to octenes for CuZ catalysts of low Brönsted acid site concentration.

Acknowledgements

The authors wish to express their appreciation to Mrs. Ágnes Wellisch for her excellent technical assistance.

REFERENCES

[1] D.C. Elliott, Energy & Fuels 21 (2007) 1792-1815.

[2] G.W. Huber, S. Iborra, A. Corma, Chem. Rev. 106 (2006) 4044-4098.

[3] D. Kubicka, Collect. Czech. Chem. Commun. 73 (2008) 1015-1044.

[4] S.N. Naik, V.V. Goud, P.K.Rout, A.K. Dalai, Renewable and Sustainable Energy Rew.14 (2010) 578-597.

[5] H.N. Chang, N.J. Kim, J. Kang, C. M. Jeong, Biotechn. Bioproc. Eng. 15 (2010) 1.

[6] J.D. Stroupe, J. Am. Chem. Soc. 71 (1949) 569.

[7] D.S. Brands, E.K. Poels, A. Bliek, Appl. Catal. A 184 (1999) 279.

[8] J.W. Evans, N.W. Cant, D.L. Trimm, M.S. Wainwright, Appl. Catal. 6 (1983) 355.

[9] Sz. Harnos, Gy. Onyestyák, J. Valyon, M. Hegedűs, Z. Károly, Proc. 10th Pannonian Int. Symp. Catal. (2010) p. 334.

[10] Gy. Onyestyák, Sz. Harnos, D. Kalló, Catal. Comm. 16 (2011) 184.

[11] M.T. Holtzapple, C.B. Granda, Appl. Biochem. Biotechnol. 156 (2009) 525.

[12] C.B. Granda, M.T. Holtzapple, G. Luce, K. Searcy, D.L. Mamrosh, Appl. Biochem. Biotechnol. 156 (2009) 537.

[13] V. Pham, M.T. Holtzapple, M.El-Halwagi, J. Ind. Microbiol. Biotechnol. 37 (2010) 1157.

[14] B.D. Cullity: in “Elements of X-ray Diffraction” 2nd Addison-Wesley Publ Co. Reading, MA, USA, 1978.

[15] H.K. Beyer, J. Papp, D. Kalló, Acta Chim. 84 (1975) 7.

Table 1. Catalyst properties

	Cu content, wt. %	[a]Degree of Cu^{2+} ion-exchange, %	[b]BET, m^2/g	[c]Cu^o particle diameter, nm
16CuA	16,4	82	8	7
15CuX	15,3	75	18	26
7CuY	7,2	71	n.d.	55
20Cu/SiAl	20,0	-	221	98

[a]Calculated from measured values: Cu^{2+} meq.g^{-1}/ (Cu^{2+} meq.g^{-1}+ Na^+ meq.g^{-1})

[b]Specific surface areas of the catalysts under pretreatment and reaction conditions.

[c]Average copper particle diameters in the catalysts after the reaction determined by XRD method.

Table 2. Comparison of commercial Adkins and the novel InCu catalysts.

	Reaction temperature	WHSV (h^{-1})	Octanal yield (wt.%)	Octanol yield (wt.%)	Conversion (wt.%)
16CuA + In_2O_3	360 °C	2	17.8	50.9	80.9
Adkins catalyst	360 °C	2	3.3	67.5	86.6
16CuA + In_2O_3	320 °C	0.5	2.7	74.9	90.3

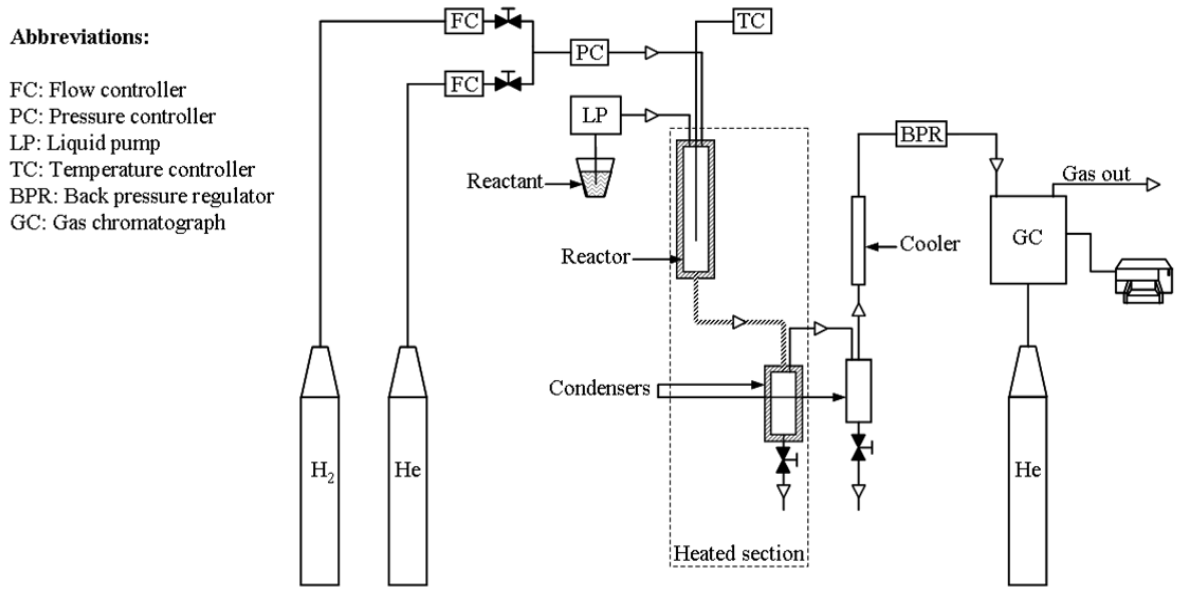

Fig. 1. A schematic figure of the high-pressure fixed bed flow reactor system.

Fig. 2.

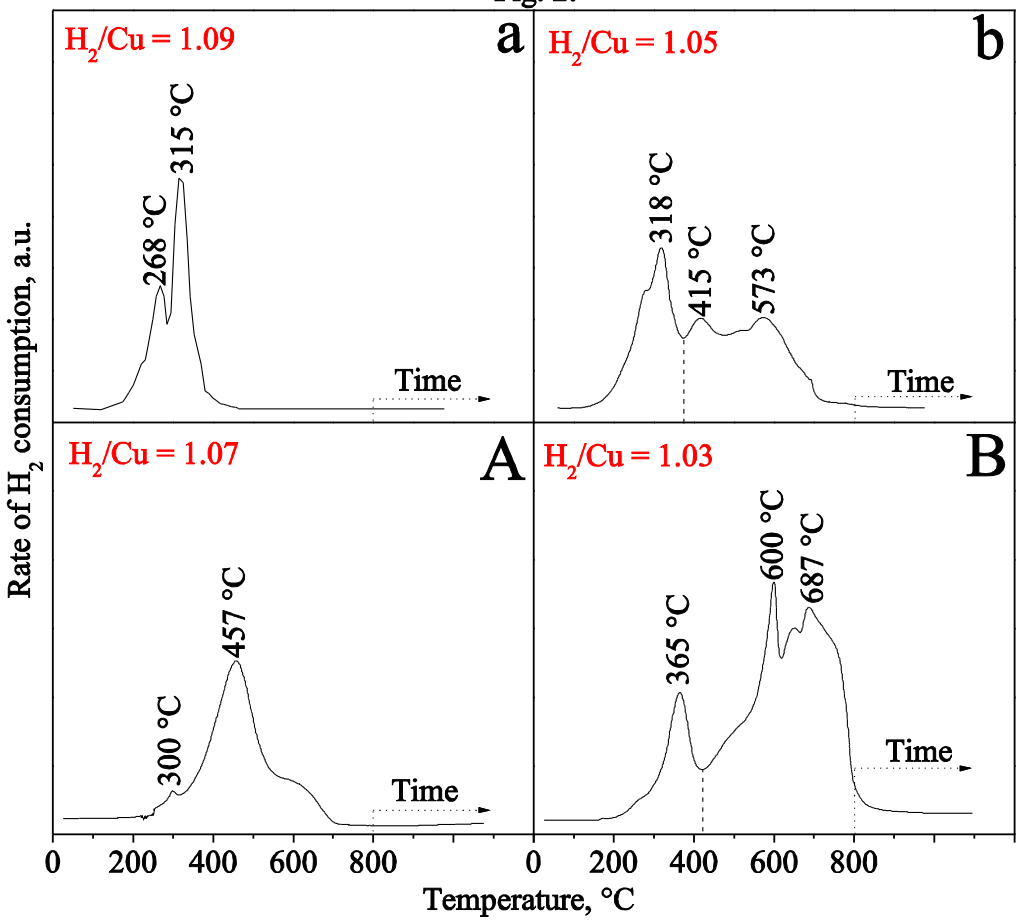

Fig. 2. H_2-TPR curves of 15CuX (a) zeolite, doped with In_2O_3 (b) and 16CuA (A) zeolite, doped with In_2O_3 (B).

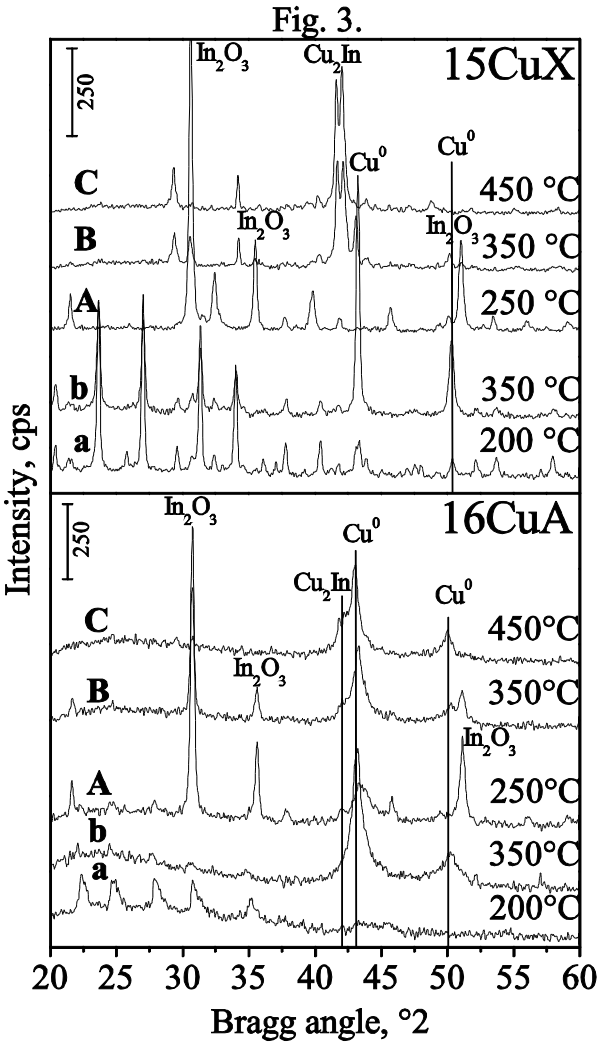

Fig. 3. HT-XRD patterns of 15CuX (upper) and 16CuA (lower) catalysts treated at different temperatures step by step up to 350 °C (a,b) and 15CuX + In_2O_3 (upper) and 16CuA + In_2O_3 (lower) to 450 °C (A, B, C) recorded in H_2 flow for half an hour.

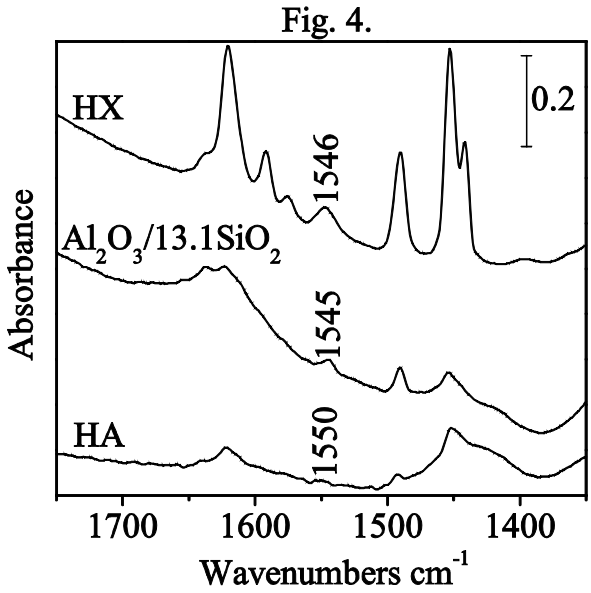

Fig. 4. IR spectra of pyridine adsorbed on deammoniated, destructed NH_4-A and -X zeolites, and 20Cu/SiAl samples after dehydration at 450 °C for 1 hour in hydrogen flow. Pyridine adsorbed on Bronsted acid sites is shown by bands at 1545-1550 cm^{-1}.

Fig. 5.

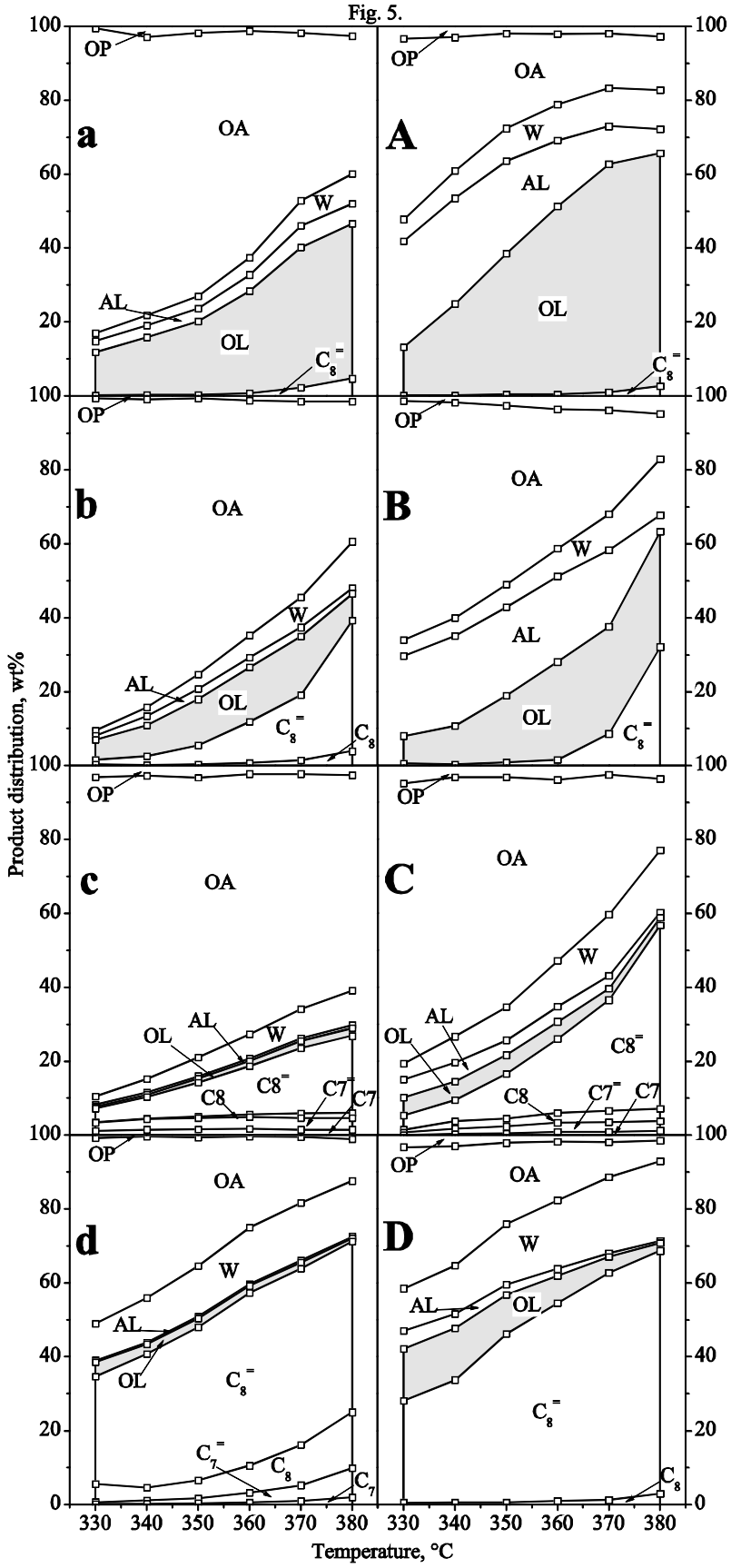
a
A
b
B
c
C
d
D
OP
OA
W
AL
OL
C8=
C8
C7=
C7
Product distribution, wt%
Temperature, °C

Fig. 5. Product distribution on 16CuA (a), 15CuX (b), 7CuY (c), 20Cu/SiAl (d) and on the same samples doped with In_2O_3 (A, B, C, D) in the hydroconversion of octanoic acid (OA) as function of reaction temperature under standard conditions using stacked area graphs. Legend: OA=octanoic acid, W= water, AL= octanal, OL=octanol, $C_8^=$ = octenes, C_8 =octane, $C_7^=$ = heptenes, C_7 = heptane, OP=other products.

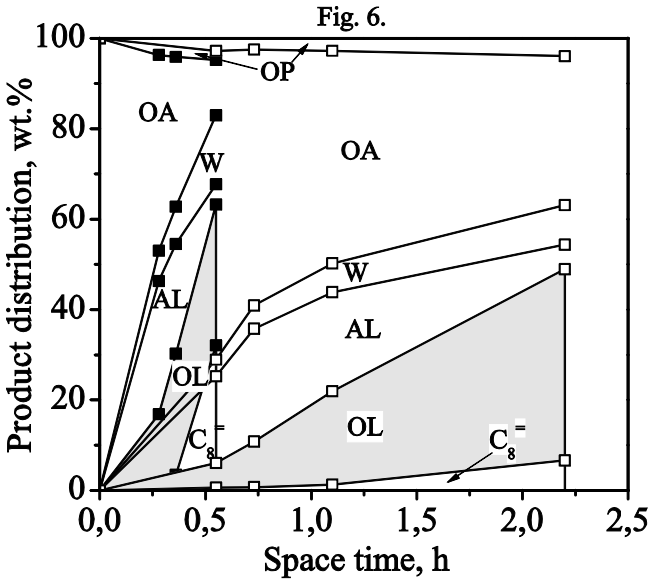

Fig. 6. Octanoic acid hydroconversion over 15CuX + In_2O_3 catalyst obtained at 320 °C (□) and 380 °C (■) as a function of space time demonstrated in stacked area graphs. Legend as in Fig. 4.

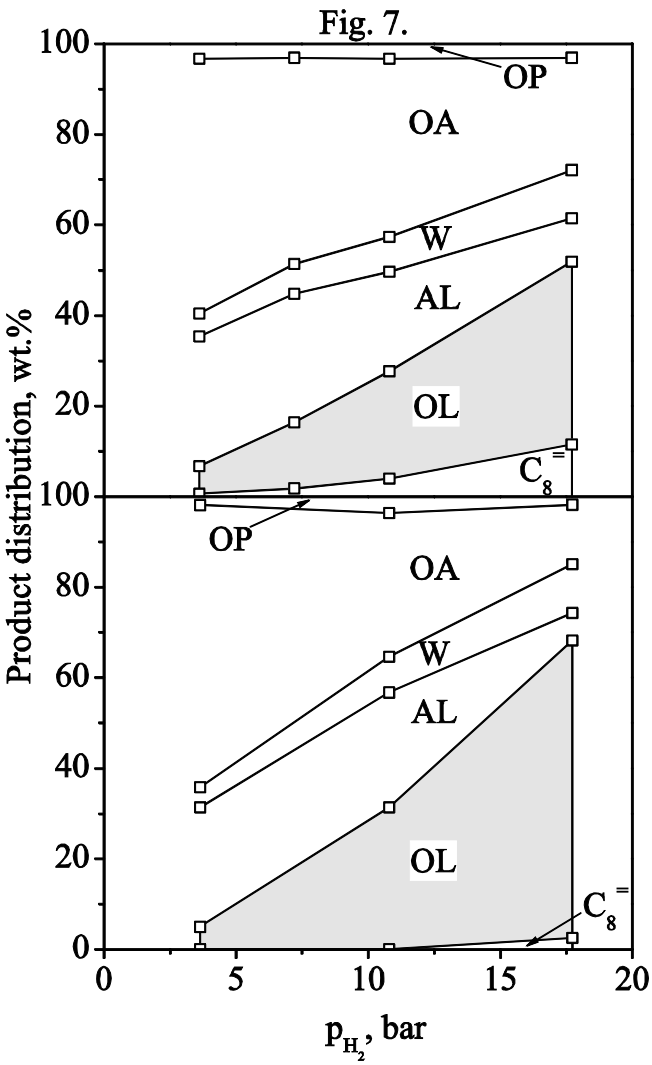

Fig. 7. Product distribution on 15CuX + In_2O_3 (upper) and 16CuA + In_2O_3 (lower) catalysts in the hydroconversion of OA/H_2/He mixture as function of hydrogen partial pressure at 380 °C. WHSV of OA was 2.0 h^{-1}. The partial pressure of OA was kept at 1.7 bar. The H_2 partial pressure was changed by changing the H_2/He ratio. Legend as in Fig. 4.

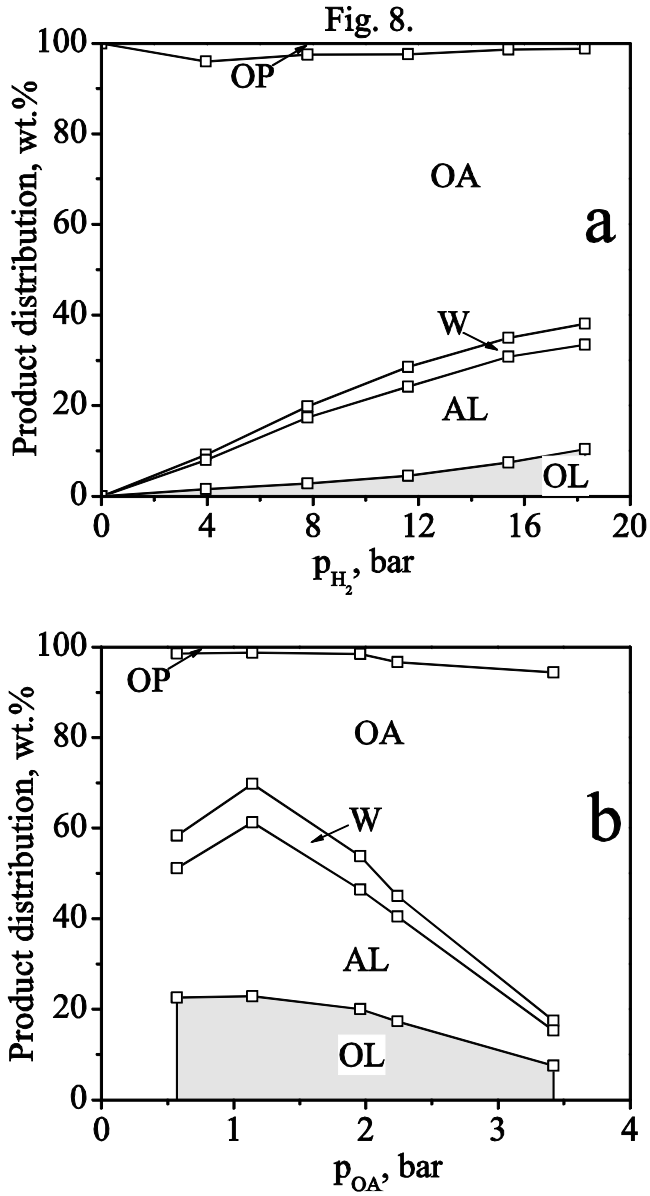

Fig. 8. Product distribution on 16CuA + In_2O_3 catalyst in the hydroconversion of OA/H_2/He mixture as function of hydrogen partial pressure (a) and as function of octanoic acid partial pressure (b) at 21 bar total pressure and 330 °C. WHSV of OA was 2.0 h^{-1}. The partial pressure of OA was kept at 1.7 bar (a) and for hydrogen at 17.7 bar (b). Legend as in Fig. 4.

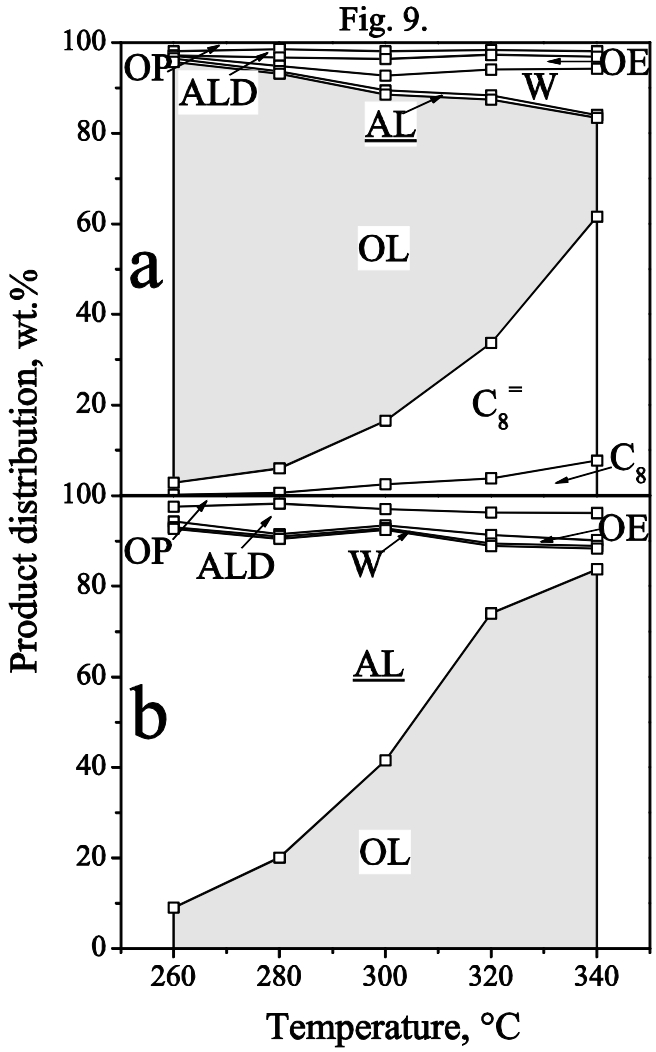

Fig. 9. Hydroconversion of octanal (AL) over 16CuA (a) and 16CuA + In_2O_3 (b) catalysts characterized by distributions of the main products between 260 and 340 °C at 21 bar total pressure using stacked area graphs. The WHSV of AL was 2.0 h^{-1}. Legend as in Fig. 4. In addition: OE =dioctyl ether, ALD = 2-hexyldec 2-enal (the product of octanal aldol condensation).

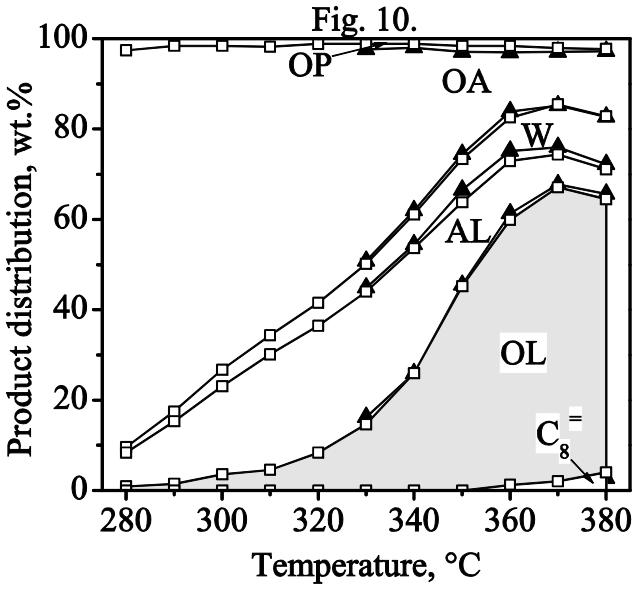

Fig.10. Hydroconversion of OA over 16CuA + 10% In_2O_3 (□) and 16CuA + 36% In_2O_3 (▲) catalysts characterized by distributions of the main products between 280 and 380 °C at 21 bar total pressure using stacked area graphs. The WHSV of OA was 2.0 h^{-1}. Legend as in Fig. 4.